stellarator news

Published by Fusion Energy Division, Oak Ridge National Laboratory
Building CR 5600 P.O. Box 2008 Oak Ridge, TN 37831-6169, USA

Editor: James A. Rome Issue 139 February 2013
E-Mail: jamesrome@gmail.com Phone (865) 482-5643
On the Web at *http://www.ornl.gov/sci/fed/stelnews*

Progress of high-temperature experiments in LHD

Realization of high-temperature plasmas is one of the most important issues in helical plasmas, which have an advantage over tokamak plasmas for steady-state operation. In the Large Helical Device (LHD), the heating capability has been upgraded year by year and the high-temperature regime has been successfully extended. In the LHD, three negative-ion-based neutral beam injectors (NBs) produce hydrogen neutral beams with a beam energy of 180 keV and a total port-through power of 16 MW [1]. These negative NBs are tangentially injected to the LHD plasma. A positive-ion-based NB [positive neutral beam injection (NBI)] with a low energy of 40 keV was perpendicularly injected for ion heating. Since 2010, a second 40-keV perpendicular NB has been operational in LHD and the total port-through power for perpendicular NBI has thus increased from 6 MW to 12 MW. An electron cyclotron resonance heating (ECRH) system with eight gyrotrons has been operated for preionization and plasma heating [2]. Enhancement of the output power per gyrotron has been planned in LHD and the replacement of the existing gyrotrons with higher-power tubes is in progress. At present, three 77-GHz gyrotrons with output power of more than 1 MW each, are operational for plasma experiments. LHD now has 28 MW of NB power and 3.7 MW of ECRH power available for experiments.

Figure 1 shows (a) the radial profiles of ion temperature T_i, electron temperature T_e, and electron density n_e in a typical high-T_i discharge with a carbon pellet, and (b) the progress of the achieved central ion temperature T_{i0} in LHD as the dependence of T_{i0} on the density-normalized ion heating power P_i/n_e, where P_i is the volume integral of the local NBI deposition power for ions evaluated using the FIT3D code, and r_{eff} in Fig. 1(a) represents the effective minor radius. Ion temperature of 7 keV at the plasma center was successfully obtained and the achieved T_{i0} has increased with P_i/n_e. High-T_i plasmas have been realized with injection of a carbon pellet [3–5]. The kinetic

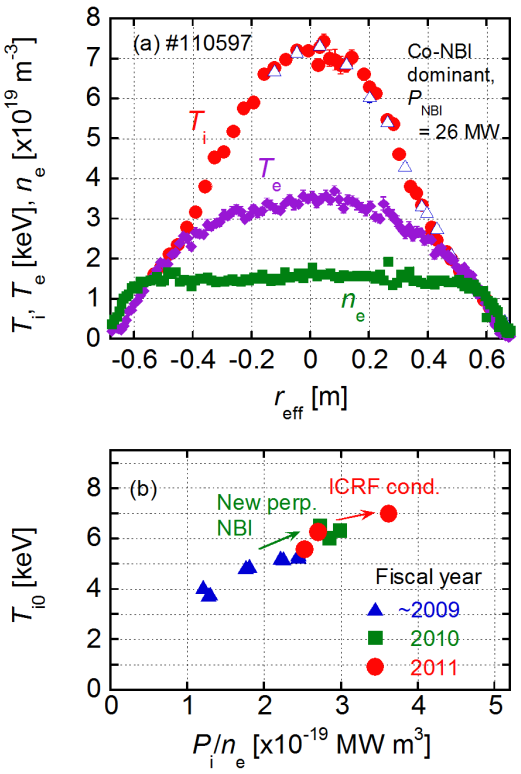

Fig. 1. (a) The radial profiles of T_i, T_e, and n_e in a typical high T_i discharge, and (b) the progress of the achieved T_i in the center of LHD.

In this issue . . .

energy confinement improves by a factor of 1.5 after pellet injection. In the high-T_i phase, a flat or hollow profile in n_e has been observed. This has different characteristics from the PEP mode investigated in tokamaks [6–8].

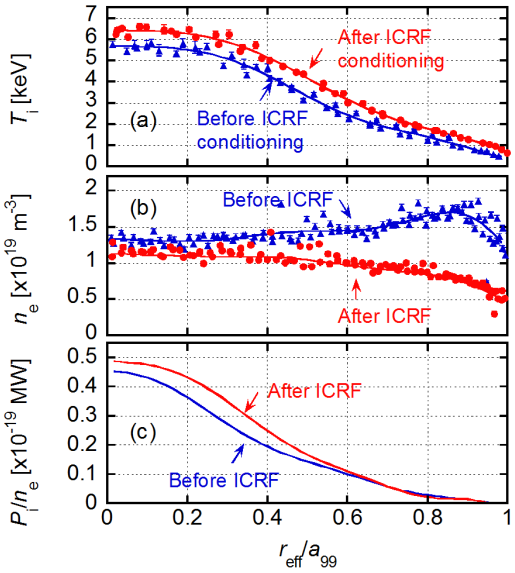

Fig. 2. Radial profiles of (a) T_i, (b) n_e, and (c) P_i/n_e before and after ICRF wall conditioning.

This improvement was attributed to the upgrade of the NB system, the optimization of the discharge scenario, and ion cyclotron radio frequency heating (ICRF) wall conditioning. It was found that intensive wall conditioning by a series of ICRF minority-ion-heating discharges helped to increase the ion temperature. In fact, there was no significant increase of NBI power from 2010 to 2011 in LHD. Figure 2 shows radial profiles of (a) T_i, (b) n_e, and (c) the ion-heating power normalized by n_e before and after ICRF conditioning. In Fig. 2, a_{99} is the averaged minor radius inside which 99% of the stored energy is confined. In the ICRF discharges, NBIs were not used and helium was fueled as the working gas for minority heating. Before the ICRF conditioning, a hollow n_e profile was formed and T_{i0} was below 6 keV. After 30 discharges of ICRF conditioning with a pulse duration of 10 s, a lower electron density with a parabolic profile and T_{i0} exceeding 6 keV were obtained. The partial pressures of both H_2 and He during the discharge were found to be decreased after ICRF wall conditioning. This represents a decrease of outgassing from the wall, namely a decrease in neutral particle recycling. The increase of T_{i0} after ICRF conditioning is considered to be the result of an increase of NBI heating power per ion at the core region due to the decrease of edge density, as can be seen from Fig. 2(c), rather than an improvement in the ion heat transport.

Figure 3 shows (a) radial profiles of T_e and n_e in a high-T_e discharge and (b) a map of simultaneously attained central electron temperature T_{e0} and line-averaged electron density for ECRH discharges. Highly accurate T_e profiles were obtained by the accumulation of the intensity of Thomson scattered light at 17 times during fixed-condition discharges with the three YAG lasers all injected together [9]. Central electron temperature of 20 keV was successfully achieved by centrally focused ECRH of 3.35 MW at an electron density of 0.2×10^{19} m^{-3}. The plasma parameter regime with regard to the electron temperature has been successfully expanded in both low- and high-density conditions.

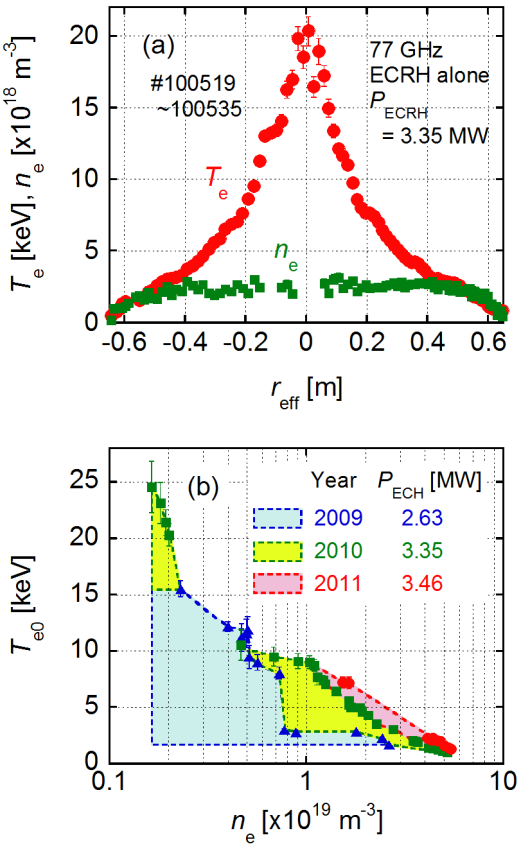

Fig. 3. (a) Radial profiles of T_e and n_e and (b) map of simultaneously attained T_{e0} and n_e for ECRH discharges.

Dynamic transport analysis that takes into account the slowing-down effect of NBI deposition is suitable when the plasma parameters change transiently in the discharge [10], as they do with the injection of a carbon [3–5]. Here the temporal changes in ion heat transport and toroidal momentum transport in high-T_i discharges are discussed. Figure 4 shows the time evolution of (a) the line-averaged electron density and the port-through NBI power, (b) the NBI absorption power, (c) the NBI input torque, (d) T_i, (e) the toroidal flow velocity V_ϕ, (f) $\chi_i/T_i^{3/2}$ at the three posi-

tions, (g) the effective viscosity μ_ϕ consisting of the tangential NB-driven rotation and the intrinsic rotation at $r_{eff}/a_{99} = 0.31$, and (h) the dependence of the Prandtl number P_r on T_i at $r_{eff}/a_{99} = 0.31$ in a typical high-T_i plasma. The thermal diffusivity is normalized by $T_i^{3/2}$ to cancel the gyro-Bohm dependence Here the Prandtl number is defined as μ_ϕ/χ_i. The integrated absorption power and the force in Figs. 4(b) and 4(c) were calculated taking account of the slowing down of the energy and the velocity of NB particles in the plasma [10]. The plasma was sustained by three tangentially injected NBs and two perpendicularly injected NBs with total-port-through power of 27 MW, and a cylindrical carbon pellet (ϕ = 1.0 mm, l = 1.0 mm) was injected at t = 4.57 s. In Ref. [3], the increment of Z_{eff} was shown to be ~1 just after carbon pellet injection, decreasing to ~0.2 due to the formation of an impurity hole. One line of the perpendicular NBs was modulated for T_i measurement by charge exchange recombinant spectroscopy (CXRS). After the pellet injection, T_i, V_ϕ, dT_i/dr_{eff} and dV_ϕ/dr_{eff}, clearly increased in the core region, indicating the formation of the ion internal transport barrier (ITB). In the core region, χ_i was found to change more slowly than in the peripheral region. The toroidal momentum transport also improved with the reduction in thermal diffusivity, and the Prandtl number (ignoring the intrinsic torque) was close to unity despite the extensive change in confinement during the discharge. Note that μ_ϕ and P_r were underestimated in this analysis by a factor of 2 at most, because the contribution of intrinsic rotation is in the co direction and peaks at r_{eff}/a_{99} ~0.6 with magnitude comparable to that driven by NBI [4]. However, the heat and the momentum confinement degraded in the latter phase of the discharge.

Figure 5 shows the flux-gradient relation between (a) Q_i/n_e and dT_i/dr_{eff} and (b) $P_\phi/n_e m_i$ and dV_ϕ/dr_{eff} at $r_{eff}/a_{99} = 0.31$, where Q_i is the ion heat flux and P_ϕ is the toroidal momentum flux [5]. The slopes in the relation between Q_i/n_e and dT_i/dr_{eff}, and between $P_\phi/n_e m_i$, and dV_ϕ/dr_{eff} correspond to χ_i and μ_ϕ, respectively. As shown in Fig. 5(a), dT_i/dr_{eff} increased after carbon pellet injection despite the small change of Q_i/n_e. This indicates that the ion heat transport was improved, leading to the achievement of 7 keV. However, the confinement improvement was temporary and dT_i/dr_{eff} gradually decreased after dT_i/dr_{eff} reached −13 keV/m. The toroidal momentum transport was also improved by ion ITB formation. The increase of dV_ϕ/dr_{eff} with constant-momentum flux means the decrease of μ_ϕ and implies an increase in intrinsic rotation. However, the momentum transport went back to the low-confinement branch in the latter phase of the dis-

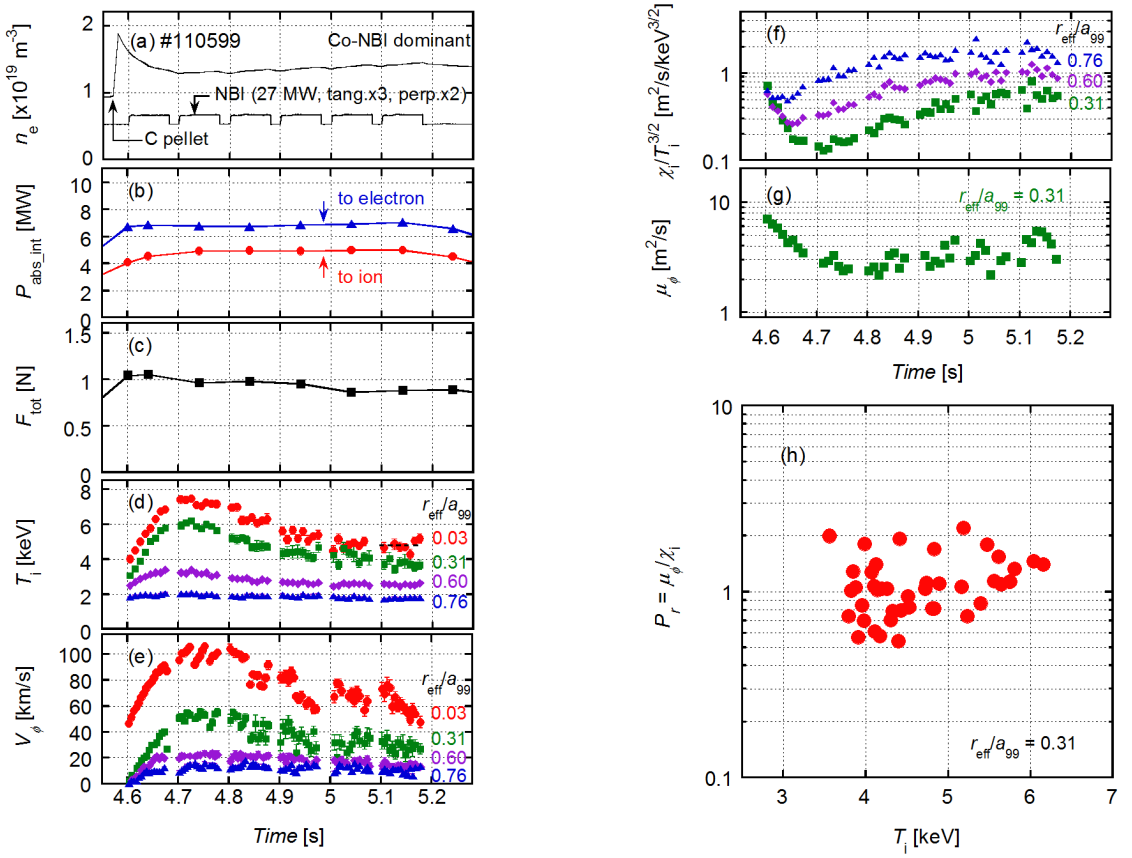

Fig. 4. The time evolution of (a) n_e, (b) the NBI absorption power, (c) the total force, (d) T_i, (e) V_ϕ, (f) $\chi_i/T_i^{3/2}$, (g) μ_ϕ, and (h) the dependence of P_r on T_i.

charge, similar to the ion heat transport. On the other hand, a change in electron heat confinement was not observed in the discharge [10]. The intrinsic rotation [5, 11] due to the off-diagonal terms in the transport matrix should be investigated for more qualitative and quantitative evaluation of heat and momentum transport. Clear dependence of the intrinsic torque on the ion temperature gradient was shown in Ref. [5]. Detailed results of the heat and momentum transport analyses, including off-diagonal terms, will be reported in the near future.

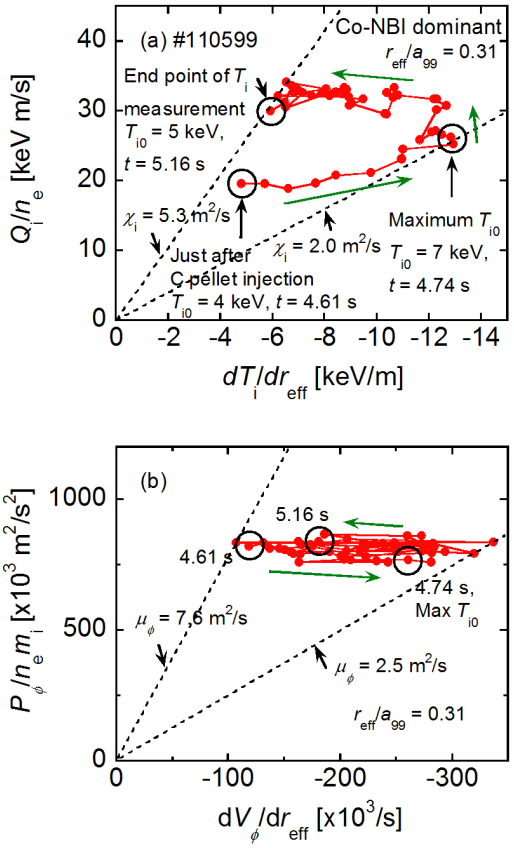

Fig. 5. The dependence of (a) Q_i/n_e on dT_i/dr_{eff} and (b) $P_\phi/n_e m_i$ on dV_ϕ/dr_{eff}.

This work was supported by NIFS grants, 11ULRR701, 11ULRR702 and ULRR703.

References

[1] Y. Takeiri et al., Fusion Sci. Technol. **58** (2010) 482.

[2] T. Shimozuma. et al., Fusion Sci. Technol. **58**, (2010) 530.

[3] K. Ida et al., Nucl. Fusion, **49** (2009) 095024.

[4] K. Ida et al., Nucl. Fusion, **50** (2010) 064007.

[5] K.Nagaoka et al., Nucl. Fusion, **51** (2011) 083022.

[6] S. Sengoku et al., Nucl. Fusion, **25** (1985) 1475.

[7] B. J. D. Tubbing et al., Nucl. Fusion, **31** (1991) 839.

[8] L. R. Baylor et al., Nucl. Fusion, **37** (1997) 127.

[9] I. Yamada et al., Rev. Sci. Instrum **81** (2010) 10D522.

[10] H. Lee et al., Plasma Phys. Control. Fusion (in press).

[11] M. Yoshinuma et al., Nucl. Fusion, **49** (2009) 075036.

Hiromi Takahashi
Plasma Heating Physics Research Division
National Institute for Fusion Science
322-6 Oroshi-cho, Toki, Gifu, 509-5292, JAPAN
E-mail: takahashi.hiromi@LHD.nifs.ac.jp